AJNR

Prognostic Value of MR and Magnetization Transfer Imaging Findings in Patients withClinically Isolated Syndromes Suggestive ofMultiple Sclerosis at Presentation

Giuseppe Iannucci, Carla Tortorella, Marco Rovaris, Maria Pia Sormani, Giancarlo Comi and Massimo Filippi

Prognostic Value of MR and Magnetization Transfer Imaging Findings in Patients with Clinically Isolated Syndromes Suggestive of Multiple Sclerosis at Presentation

Giuseppe Iannucci, Carla Tortorella, Marco Rovaris, Maria Pia Sormani, Giancarlo Comi, and Massimo Filippi

BACKGROUND AND PURPOSE: The extent of abnormalities on T2-weighted MR images of the brain of patients with clinically isolated syndromes (CIS) suggestive of multiple sclerosis (MS) at presentation is associated with an increased risk of developing clinically definite MS (CDMS). We evaluated whether subtle changes outside T2-visible lesions are present in the brain of these patients and whether their extent increases the risk of subsequent development of CDMS.

METHODS: Dual-echo, T1-weighted, and magnetization transfer (MT) images of the brain were obtained from 24 patients with CIS at presentation. These patients were followed up for a mean period of 33 months (range, 25–42 months). Twenty age- and sex-matched healthy volunteers served as control subjects. To create MT histograms of the normal-appearing brain tissue (NABT), macroscopic lesions were segmented from dual-echo images, were superimposed automatically, and were nulled out from the coregistered and scalp-stripped MT ratio (MTR) maps. The following MTR histogram-derived measures were considered: average MTR, MTR_{25}, MTR_{50}, MTR_{75}, peak height, and peak position. T2 and T1 lesion loads, average lesion MTR, and brain volume were also measured.

RESULTS: Patients with CIS had lower average NABT-MTR ($P < .0001$) and peak position ($P = .002$) than did control volunteers, but patient brain size was similar to that of volunteers. At follow-up, 10 (41%) patients developed CDMS. Patients who developed CDMS during the follow-up period had higher T2 lesion volume ($P = .003$) and lower average NABT-MTR ($P = .005$) and peak position ($P = .006$) than did those who did not develop CDMS. T2 lesion volume (odd ratio, 3.54; $P = .0005$) and average NABT-MTR (odd ratio, 0.81; $P = .01$) were independent predictors of the subsequent development of CDMS.

CONCLUSION: Subtle changes occur outside lesions visible on conventional MR images among patients with CIS suggestive of MS at presentation. The greater the extent of such abnormalities is, the higher is the risk of subsequent development of CDMS.

T2-weighted MR imaging of the brain reveals multifocal asymptomatic white matter abnormalities in 50% to 70% of patients with clinically iso-lated syndromes (CIS) suggestive of multiple sclerosis (MS) (1–17). These abnormalities are indistinguishable from those seen in cases of clinically definite MS (CDMS), and their presence and extent markedly increase the risk of developing CDMS (5–17).

In patients with CDMS, microscopic changes in the white matter outside T2-visible lesions are frequently detected using several MR techniques, including magnetization transfer (MT) imaging (18–24). In this study, we obtained MT ratio (MTR) histograms of the normal-appearing brain tissue (NABT) to evaluate whether changes outside T2-visible lesions are seen in the brain of patients with CIS at presentation and to assess whether their extent increases the likelihood of subsequent development of CDMS.

Methods

Patients

We performed MR imaging of the brain in all patients presenting with CIS suggestive of MS between August 1995 and February 1997. In addition to the criteria previously used to select patients with CIS at presentation for prognostic studies (12, 14, 15, 17), we required that the patients had to have at least four T2 lesions of the type seen in cases of CDMS or only three of such lesions if one of them was either subcortical or infratentorial. This was to minimize the chance of recruiting patients with neurologic conditions other than MS, as shown by a recent prospective study (25). When MR images were obtained, a full neurologic assessment was conducted by a single observer who was unaware of the MR findings, and the disability was rated using the Expanded Disability Status Scale score (26). Patients were then prospectively followed up by the same neurologists, with visits scheduled every 6 months, or when the patients experienced new symptoms. The followup duration was a mean of 33 months (range, 25–42 months). During the follow-up period, MS was diagnosed solely on clinical grounds by using the Poser criteria (27); paraclinical data were not used. Twenty sex- and age-matched control volunteers (eight men and 12 women; mean age, 33.8 years; SD, 5.0 years) with no history of neurologic diseases and with normal results of their neurologic examinations were also studied. Local Ethical Committee approval and written informed consent from all the patients and control volunteers were obtained before study initiation.

Image Acquisition

MR images of the brain were obtained using an imager operating at 1.5 T. During a single session, the following images were obtained: dual-echo spin-echo (2400/30, 80/1 [TR/TE/excitations]); T1-weighted spin-echo (768/15/2); and 2D gradient-echo (600/12, $\alpha = 20°$), with and without an MT saturation pulse. The RF saturation pulse was 1.5 kHz below the water frequency, with a gaussian envelope of duration of 16.4 ms, a bandwidth of 250 Hz, and an amplitude of 3.4×10^{-6} T. For the dual-echo and T1-weighted images, 24 contiguous, interleaved, axial sections were acquired with 5-mm section thickness, a 256×256 matrix, and a 250×250-mm field of view. MT images were obtained using the same acquisition parameters, except for the number of sections, which was 20. The set of sections for the MT images was positioned to obtain the same central 20 sections as for the dual-echo and T1-weighted images. The sections were positioned to run parallel to a line that joins the most inferoanterior and inferoposterior parts of the corpus callosum, according to published guidelines (28).

Image Analysis

Lesions were first identified by agreement between two experienced observers who did not know to whom the images belonged, on the dual-echo and T1-weighted hard copies, following a procedure described elsewhere (29). Using four contiguous T1-weighted sections, with the most caudal section at the level of the velum interpositum cerebri (30), we calculated an MR measure of cerebral volume. Brain and lesion volume measurements were obtained by a single observer, who did not know to whom the images belonged, using a semiautomated segmentation technique based on local thresholding (29).

From the two gradient-echo images, with and without the saturation pulse, and after their coregistration, MTR maps were derived pixel-by-pixel, as previously described (29). Lesion outlines on proton density–weighted images were superimposed onto the coregistered MTR maps and average lesion MTR was calculated. We also derived MTR histograms (with bins 1% in width) for the NABT (ie, the overall brain tissue not involved by lesions visible on the dual-echo images). First,

we removed the skull and other extracranial tissues from the proton density– and gradient-echo images without and with the MT pulse, using the same local thresholding technique as that used for lesion segmentation (29). Second, the scalp-stripped gradient-echo images were coregistered and MTR maps obtained. The MTR maps were then coregistered with the corresponding scalp-stripped proton density–weighted images. Coregistration of images was performed using a surface-matching technique that fits the contours corresponding to the CSF-dura interface of the two MR images (31, 32). Finally, the macroscopic lesions segmented on proton density–weighted images were superimposed automatically onto the coregistered MTR map, and the areas corresponding to the segmented lesions were nulled. For comparability of results, the entire procedure, except the removal from the MTR maps of the tissue belonging to macroscopically visible T2 lesions, was performed also for the images of the control volunteers. To minimize the inclusion of pixels with partial volume averaging from the CSF, we excluded from the analysis all the pixels with MTR values lower than 10%. To correct for the between-patient differences in brain volume, each histogram was normalized by dividing it by the total number of pixels included. For each histogram, several parameters were analyzed: the height and the position of the histogram peak, with respect to the x axis, the average MTR value, and the MTR values corresponding to the 25th, 50th, and 75th percentiles of the histogram (ie, MTR_{25}, MTR_{50}, and MTR_{75}) that indicate the MTR value at which the integral of the histogram is 25%, 50%, and 75% of the total, respectively.

Statistical Analysis

Differences in MR and MT imaging metrics between patients and control volunteers and between patients who developed CDMS and those who did not were evaluated using a two-tailed Student's t test for nonpaired data. A multivariate analysis with a logistic model was conducted to evaluate the MR and MT imaging variables that independently influenced the probability of patients developing CDMS. The independent variables included in the model were the hyperintense T2 lesion load, the hypointense T1 lesion load, the average lesion MTR, and the average MTR of the NABT.

Results

Twenty-four patients (11 men and 13 women) were included in the study. The mean patient age was 27.2 years (SD, 5.6 years), the mean duration between clinical onset and MR acquisition was 16 days (range, 3–38 days), and the median Expanded Disability Status Scale score was 1.0 (range, score of 0.0–1.5). Ten patients had isolated syndrome of the brain, nine had unilateral acute optic neuritis, and five had isolated spinal cord syndrome. In all patients, CSF analysis was also conducted. CSF oligoclonal bands were found in 20 (83%) patients. At follow-up, 10 (41%) patients (four men and six women) developed CDMS. There were no significant differences in any of the baseline clinical characteristics among patients with different clinical presentations or between those who did and did not develop CDMS during the follow-up period. At follow-up, the median Expanded Disability Status Scale score was 0.5 for patients who did not develop CDMS and 1.5 for patients who did (P = not significant).

No abnormalities were found on the images of the control volunteers. In the entire cohort of patients with CIS, the mean hyperintense T2 lesion volume was 6.3 mL (range, 0.6–25.4 mL), the mean hypointense T1 lesion volume was 0.2 mL (range, 0.0–1.0 mL), and the average lesion MTR was 40.5% (SD, 2.0%). No significant differences in any of the MR or MT imaging–derived metrics studied were found among patients with different clinical presentations. In Table 1, the hyperintense T2 and hypointense T1 lesion volumes together with average lesion MTR for the patients who developed

TABLE 1: Lesion loads on T2- and T1-weighted scans and average lesion MTR at presentation in patients not developing and developing CDMS

	Patients Not Developing CDMS	Patients Developing CDMS	P*
Mean (SD) T_2 lesion load (mL)	3.8 (1.9)	9.8 (6.3)	.003
Mean (SD) T_1 lesion load (mL)	0.1 (0.2)	0.3 (0.3)	N.S.
Average lesion MTR (SD) (%)	41.0 (2.1)	39.9 (1.5)	N.S.

* Statistical analysis: two-tailed Student's t test for non-paired data; N.S. = not significant.

TABLE 2: MTR histogram metrics in the NABT from control subjects and patients with CIS at presentation

	Control Subjects	CIS	P*
Average MTR (SD) (%)	49.8 (0.9)	48.6 (0.9)	<.0001
Mean MTR_{25} (SD) (%)	41.9 (0.9)	40.5 (1.1)	<.0001
Mean MTR_{50} (SD) (%)	44.3 (1.2)	43.0 (1.2)	.001
Mean MTR_{75} (SD) %	46.3 (1.1)	44.9 (1.2)	<.0001
Mean peak height (SD)	126.8 (10.7)	129.1 (10.8)	N.S.
Mean peak position (SD) (%)	45.0 (1.2)	43.8 (1.2)	.002

* Statistical analysis: two-tailed Student's t test for non-paired data; N.S. = not significant.

TABLE 3: NABT-MTR histogram metrics at presentation in patients not developing and developing CDMS

	Patients Not Developing CDMS	Patients Developing CDMS	P*
Average MTR (SD) (%)	49.1 (0.8)	48.0 (0.8)	.005
Mean MTR_{25} (SD) (%)	41.0 (1.0)	39.8 (1.0)	.01
Mean MTR_{50} (SD) (%)	43.5 (1.0)	42.2 (1.0)	.006
Mean MTR_{75} (SD) (%)	45.5 (1.0)	44.2 (1.0)	.006
Mean peak height (SD)	127.7 (10.3)	131.2 (11.5)	N.S.
Mean peak position (SD) (%)	44.4 (0.8)	43.1 (1.2)	.006

* Statistical analysis: two-tailed Student's t test for non-paired data; N.S. = not significant.
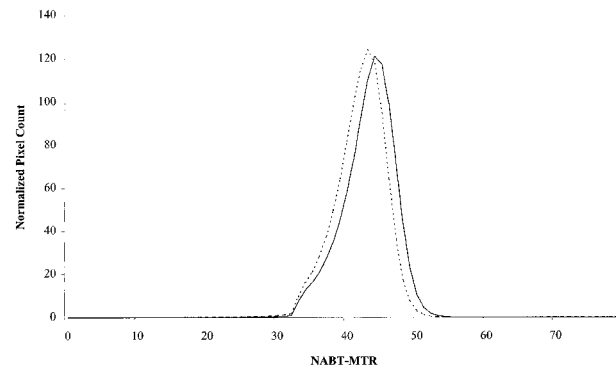

FIG 1. MTR histograms of the NABT of patients with CIS at presentation who developed CDMS during the follow-up period (*continuous line*) and of patients with CIS at presentation who did not develop CDMS during the follow-up period (*dotted line*).

average NABT-MTR (odd ratio, 0.81; $P = .01$) were independent predictors of the subsequent development of CDMS. All the other factors were excluded from the multiple regression model.

Discussion

This study shows that microscopic changes outside T2-visible lesions do occur in patients with CIS suggestive of MS at presentation and that the greater their extent is, the higher is the risk of subsequent development of new neurologic symptoms leading to a diagnosis of CDMS.

Previous pathologic studies (33–35) indicated that astrocytic hyperplasia, patchy edema, perivascular infiltration, abnormally thin myelin, and axonal loss can occur in the brain white matter outside macroscopic lesions of patients with MS. All these abnormalities can modify the relative proportions of mobile and immobile protons of the diseased tissue and, as a consequence, determine a decrease of its MTR. Previous studies have found decreased MTR values in small regions of the brain spared by T2-visible lesions from patients with CDMS (18–22). In the present study, we obtained MTR histograms of the overall NABT from patients with CIS at presentation, by accurately removing from the coregistered MTR maps all the pixels known to belong to T2-visible lesions. Because normal-appearing white matter represents the largest part of NABT included in our MTR histograms, we think that microscopic white matter abnormalities rather than abnormalities in the gray matter (ie, cerebral and cerebellar cortex and basal ganglia) may be responsible for the differences in MTR histogram–derived metrics between patients with CIS at presentation and control volunteers. Nevertheless, it is clear that lesions in or adjacent to the cerebral cortex, which can be imaged using fast fluid-attenuated inversion-recovery sequences (36–38), may have been missed in the present study and may also have contributed to the MTR histogram findings. On the contrary, the role of pathologic changes in the basal ganglia is likely to be minor, if present at all, because of the low fre-

CDMS during the follow-up period and those who did not are reported. Patients who developed CDMS during the follow-up period had significantly higher T2 and T1 lesion volumes and significantly lower average lesion MTR than did those who did not develop CDMS. The mean brain volume was 386 mL (SD, 20 mL) for control volunteers, 384 mL (SD, 36 mL) for patients with CIS and no further clinical evolution, and 356 mL (SD, 20 mL) for patients with CIS who subsequently developed CDMS (these differences were not statistically significant).

In Table 2, NABT-MT metrics from control volunteers and the entire cohort of patients with CIS are reported. Patients with CIS had significantly lower average NABT-MTR, MTR_{25}, MTR_{50}, MTR_{75}, and peak position than did control volunteers. In Table 3, NABT-MT metrics from patients who developed CDMS during the follow-up period and from those who did not are reported. In Figure 1, the mean NABT-MTR histograms for the two groups of patients are presented. Patients developing CDMS had significantly lower average NABT-MTR, MTR_{25}, MTR_{50}, MTR_{75}, and peak position than did those who did not develop CDMS. The multivariate analysis showed that the T2 lesion volume (odd ratio, 3.54; $P = .0005$) and the

quency of clinical (39) or MR (40) involvement of these structures, even in patients with CDMS.

Previous studies showed that the presence and extent of T2 lesions are associated with an increased risk of developing CDMS in subsequent years (5–17). This study confirms these observations and shows that, in patients with CIS at presentation and on MR images suggestive of MS (25), microscopic changes occurring outside T2-visible lesions also influence the subsequent evolution of the disease. Although not confirmed by all (41), previous studies showed that MTR (21, 42) or MR spectroscopy (43) changes can be detected in the normal-appearing white matter subsequently involved by new MS lesions. Although MTR histogram analysis is inevitably not sensitive to a small amount of disease in the NABT, our results suggest that the larger the extent of microscopic abnormalities that can act as foci for the development of new macroscopic lesions is, the greater is the risk that one of these is located in a clinically eloquent area and, as a consequence, is liable to determine new neurologic symptoms. Admittedly, the presence of enhancing lesions on MR images of patients with CIS at presentation is also an important predicting factor of subsequent conversion to CDMS (25). In the present study, however, we did not obtain contrast-enhanced MR images, because some, but not all, patients received different regimens of steroid treatment during the time elapsing between clinical presentation and MR acquisition. This would have inevitably confounded the results when evaluating the presence and extent of contrast enhancement.

We also assessed the degree and amount of tissue damage within macroscopic lesions from patients with CIS by measuring the average lesion MTR and the hypointense T1 lesion load. In patients with relapsing-remitting or secondary-progressive MS, the average lesion MTR tends to be lower than that which we found in our patients with CIS (29) and the proportion of hypointense T1 lesions is higher (44, 45) (ie, approximately 15–30% versus approximately 2% in the present study). The paucity and mildness of intrinsic lesion damage may be why it does not seem to have a relevant influence on the subsequent disease course. The paucity of macroscopic lesions seen in patients with CIS also suggests that the subtle changes potentially responsible for our MTR histogram findings are at least partially independent of larger abnormalities rather than being secondary to the damage of axons traversing macroscopic lesions and resulting in Wallerian degeneration in areas away from them.

References

1. Ormerod IEC, McDonald WI, du Boulay EPGH, et al. **Disseminated lesions at presentation with optic neuritis.** *J Neurol Neurosurg Psychiatry* 1986;49:124–127
2. Ormerod IEC, Bronstein AM, Rudge P, et al. **Magnetic resonance imaging in clinically isolated lesions of the brainstem.** *J Neurol Neurosurg Psychiatry* 1986;49:737–743
3. Jacobs L, Kinkel PR, Kinkel WR. **Silent brain lesions in patients with isolated optic neuritis. A clinical and nuclear magnetic resonance study.** *Arch Neurol* 1986;43:452–455
4. Miller DH, McDonald WI, Blumhardt LD, et al. **Magnetic resonance imaging in isolated non-compressive spinal cord syndromes.** *Ann Neurol* 1987;22:714–723
5. Miller DH, Ormerod IEC, Rudge P, et al. **The early risk of multiple sclerosis following acute syndromes of the brain-stem and spinal cord.** *Ann Neurol* 1989;26:635–639
6. Ford B, Tampieri D, Francis G. **Long-term follow-up of acute partial transverse myelopathy.** *Neurology* 1992;42:250–252
7. Paty DW, Oger JJF, Kastrukoff LF, et al. **MRI in the diagnosis of MS: a prospective study with comparison of clinical evaluation, evoked potentials, oligoclonal banding, and CT.** *Neurology* 1988;38:180–185
8. Miller DH, Ormerod IEC, McDonald WI, et al. **The early risk of multiple sclerosis after optic neuritis.** *J Neurol Neurosurg Psychiatry* 1988;51:1569–1571
9. Frederiksen JL, Larsson HBW, Olesen J, Stigsby B. **MRI, VEP, SEP and biothesiometry suggest monosymptomatic acute optic neuritis to be a first manifestation of multiple sclerosis.** *Acta Neurol Scand* 1991;83:343–350
10. Lee KH, Hashimoto SA, Hooge JP, et al. **Magnetic resonance imaging of the head in the diagnosis of multiple sclerosis: a prospective 2-year follow-up with comparison of clinical evaluation, evoked potentials, oligoclonal banding and CT.** *Neurology* 1991;41:657–660
11. Martinelli V, Comi GC, Filippi M, et al. **Paraclinical tests in acute-onset optic neuritis: basal data and results of a short follow-up.** *Acta Neurol Scand* 1991;84:231–236
12. Morrissey SP, Miller DH, Kendall BE, et al. **The significance of brain magnetic resonance imaging abnormalities at presentation with clinically isolated syndromes suggestive of multiple sclerosis: a 5-year follow up study.** *Brain* 1993;116:135–146
13. Beck RW, Arrington J, Murtagh FR, Cleary PA, Kaufman DI. **Brain magnetic resonance imaging in acute optic neuritis: experience of the Optic Neuritis Study Group.** *Arch Neurol* 1993;50:841–846
14. Filippi M, Horsfield MA, Morrissey SP, et al. **Quantitative brain MRI lesion load predicts the course of clinically isolated syndromes suggestive of multiple sclerosis.** *Neurology* 1994;44:635–641
15. O'Riordan JI, Thompson AJ, Kingsley DP, et al. **The prognostic value of brain MRI in clinically isolated syndromes of the CNS: a 10-year follow-up.** *Brain* 1998;121:495–503
16. Söderström M, Ya-Ping J, Hillert J, Link H. **Optic neuritis: prognosis for multiple sclerosis from MRI, CSF, and HLA findings.** *Neurology* 1998;50:708–714
17. Sailer M, O'Riordan JI, Thompson AJ, et al. **Quantitative MRI in patients with clinically isolated syndromes suggestive of demyelination.** *Neurology* 1999;52:599–606
18. Dousset V, Grossman RI, Ramer KN, et al. **Experimental allergic encephalomyelitis and multiple sclerosis: characterization with magnetization transfer imaging.** *Radiology* 1992;182:483–491
19. Filippi M, Campi A, Dousset V, et al. **A magnetization transfer imaging study of normal-appearing white matter in multiple sclerosis.** *Neurology* 1995;45:478–482
20. Loevner LA, Grossman RI, Cohen JA, Lexa FJ, Kessler D, Kolson DL. **Microscopic disease in normal-appearing white matter on conventional MR images in patients with multiple sclerosis: assessment with magnetization-transfer measurements.** *Radiology* 1995;96:511–515
21. Filippi M, Rocca MA, Martino G, Horsfield MA, Comi G. **Magnetization transfer changes in the normal appearing white matter precede the appearance of enhancing lesions in patients with multiple sclerosis.** *Ann Neurol* 1998;43:809–814
22. Filippi M, Rocca MA, Minicucci L, et al. **Magnetization transfer of clinically or laboratory supported definite MS patients with negative conventional MRI scans.** *Neurology* 1999;52:588–594
23. Barbosa S, Blumhardt LD, Roberts N, Lock T, Edwards RH. **Magnetic resonance relaxation time mapping in multiple sclerosis: normal appearing white matter and the "invisible" lesion load.** *Magn Reson Med* 1994;12:33–42
24. Fu L, Matthews PM, De Stefano N, et al. **Imaging axonal damage of normal-appearing white matter in multiple sclerosis.** *Brain* 1998;121:103–113
25. Barkhof F, Filippi M, Miller DH, et al. **Comparison of MRI criteria at first presentation to predict conversion to clinically definite multiple sclerosis.** *Brain* 1997;120:2059–2069

26. Kurtzke JF. **Rating neurological impairment in multiple sclerosis: an expanded disability status scale (EDSS).** *Neurology* 1983;33:1444–1452

27. Poser CM, Paty DW, Scheinberg L, et al. **New diagnostic criteria for multiple sclerosis: guidelines for research protocols.** *Ann Neurol* 1983;13:227–231

28. Miller DH, Barkhof F, Berry I, Kappos L, Scotti G, Thompson AJ. **Magnetic resonance imaging in monitoring the treatment of multiple sclerosis: Concerted Action Guidelines.** *J Neurol Neurosurg Psychiatry* 1991;54:683–688

29. Filippi M, Iannucci G, Tortorella C, et al. **Comparison of MS clinical phenotypes using conventional and magnetization transfer MRI.** *Neurology* 1999;52:588–594

30. Losseff NA, Wang L, Lai HM, et al. **Progressive cerebral atrophy in multiple sclerosis: a serial MRI study.** *Brain* 1996; 119:2009–2019

31. Jiang H, Robb R, Holton KS. **A new approach to 3-D registration of multimodality medical images by surface matching.** *Proc SPIE* 1992;1808:196–213

32. West J, Fitzpatrick JM, Wang MY, et al. **Comparison and evaluation of retrospective intermodality brain image registration techniques.** *J Comput Assist Tomogr* 1997;21:554–566

33. Adams CMW. **Pathology of multiple sclerosis: progression of the lesion.** *Br Med Bull* 1977;33:15–20

34. Allen IV, McKeown SR. **A histological, histochemical and biochemical study of the macroscopically normal white matter in multiple sclerosis.** *J Neurol Sci* 1979;41:81–91

35. Trapp BD, Peterson J, Ransohoff RM, Rudick R, Mörk S, Bö L. **Axonal transection in the lesions of multiple sclerosis.** *N Engl J Med* 1998;338:278–285

36. Hashemi RH, Bradley WG, Chen DY, et al. **Suspected multiple sclerosis: MR imaging with a thin-section fast-FLAIR pulse sequence.** *Radiology* 1995;196:505–510

37. Filippi M, Yousry TA, Baratti C, et al. **Quantitative assessment of MRI lesion load in multiple sclerosis: a comparison of conventional spin-echo with fast fluid-attenuated inversion recovery.** *Brain* 1996;119:1349–1355

38. Gawne-Cain ML, O' Riordan JI, Thompson AJ, Moseley IF, Miller DH. **Multiple sclerosis lesion detection in the brain: a comparison of fast fluid-attenuated inversion recovery and conventional T2-weighted dual spin-echo.** *Neurology* 1997;49:364–370

39. Compston A, Ebers G, Lassmann H, McDonald I, Matthews B, Wekerle H. **Symptoms and signs of multiple sclerosis.** McAlpine's Multiple sclerosis. London: Churchill Livingstone;1998;

40. Grimaud J, Millar J, Thorpe JW, Moseley IF, McDonald WI, Miller DH. **Signal intensity on MRI of basal ganglia in multiple sclerosis.** *J Neurol Neurosurg Psychiatry* 1995;59:306–308

41. Silver NC, Lai M, Symms MR, Barker GJ, McDonald WI, Miller DH. **Serial magnetization transfer imaging to characterize the early evolution of new MS lesions.** *Neurology* 1998;51:758–764

42. Goodkin DE, Rooney WD, Sloan R, et al. **A serial study of new MS lesions and the white matter from which they arise.** *Neurology* 1998;51:1689–1697

43. Narayana PA, Doyle TJ, Lai D, Wolinsky JS. **Serial proton magnetic resonance spectroscopic imaging, contrast-enhanced magnetic resonance imaging, and quantitative lesion volumetry in multiple sclerosis.** *Ann Neurol* 1998;43:56–71

44. van Walderveen MA, Barkhof F, Hommes OR, et al. **Correlating MRI and clinical disease activity in multiple sclerosis: relevance of hypointense lesions on short-TR/short-TE (T1-weighted) spin-echo images.** *Neurology* 1995;45:1684–1690

45. Filippi M, Rocca MA, Horsfield MA, et al. **Increased spatial resolution using a three-dimensional T1-weighted gradient-echo MR sequence results in greater hypointense lesion volumes in multiple sclerosis.** *AJNR Am J Neuroradiol* 1998;19: 235–238